Microjoule-energy, 1 MHz repetition rate pulses from all-fiber-integrated nonlinear chirped-pulse amplifier

H. Kalaycioglu,[1,*] B. Oktem,[2] Ç. Şenel,[1] P. P. Paltani,[1] and F. Ö. Ilday[1]

[1]*Physics Department, Bilkent University, Çankaya, Ankara 06800, Turkey*
[2]*Material Science and Nanotechnology Graduate Program, Bilkent University, Ankara 06800, Turkey*
**Corresponding author: hamitkal@bilkent.edu.tr*

Received February 11, 2010; accepted February 16, 2010;
posted March 2, 2010 (Doc. ID 124188); published March 23, 2010

We demonstrate generation of pulses with up to 4 μJ energy at 1 MHz repetition rate through nonlinear chirped-pulse amplification in an entirely fiber-integrated amplifier, seeded by a fiber oscillator. The peak power and the estimated nonlinear phase shift of the amplified pulses are as much as 57 kW and 22π, respectively. The shortest compressed pulse duration of 140 fs is obtained for 3.1 μJ of uncompressed amplifier output energy at 18π of nonlinear phase shift. At 4 μJ of energy, the nonlinear phase shift is 22π and compression leads to 170-fs-long pulses. Numerical simulations are utilized to model the experiments and identify the limitations. Amplification is ultimately limited by the onset of Raman amplification of the longer edge of the spectrum with an uncompressible phase profile.

OCIS codes: 060.2320, 320.7090, 060.3510.

There is much worldwide interest in the development of powerful, robust, and simple-to-operate ultrafast fiber lasers. Their biggest drawback is the limitation to peak power by nonlinear effects. While most efforts are focused on weakening these effects through the use of large core specialty fibers [1], another approach is to manage the nonlinear effects. Examples of this approach include proposals on direct compensation of nonlinear effects [2], mitigation by spectral preshaping [3], and indirect compensation via third-order dispersion [4–6]. The latter, also known as nonlinear chirped-pulse amplification (nonlinear CPA), has led to the generation of 30 μJ, 240 fs pulses [7] and 100 μJ, 650 fs pulses [5] using 40-μm-core specialty photonic crystal fibers, along with 100 μJ, 270 fs pulses [8] using a 80-μm-core rod-type amplifier. The main advantages of nonlinear CPA are that it enables generation of short pulses from a fiber-stretcher, grating-compressor pair with unmatched third-order dispersion and allows the accumulation of significant nonlinear phase shift. The main drawback is that pulse quality is significantly reduced. Nevertheless, this is acceptable for many applications based on peak power, where pulse quality is of secondary concern.

To date, all implementations of nonlinear CPA producing high-energy pulses have relied on the use of specialty Yb-doped fibers with extremely large core diameters requiring the use of bulk optics to couple signal and pump light into the fiber. Although these fibers allow higher energies to be generated, they require special preparation of the fiber ends and much care in bulk coupling of pump light and maintaining single-mode operation. These aspects negate some of the primary advantages of fiber amplifiers. To make full use of the advantages of the nonlinear CPA approach, the entire amplifier should be implemented in fiber. Recently, we demonstrated a 10 W fiber amplifier at 40 MHz repetition rate, where pulse propagation from fiber oscillator until the grating compressor was in fiber [9].

Here, we demonstrate an all-fiber-integrated nonlinear CPA system, seeded by a fiber oscillator, generating pulses with energy up to 4 μJ at 1 MHz repetition rate. The integrated architecture allows truly robust long-term operation. The shortest dechirped pulse duration of 140 fs is obtained for 3.1 μJ amplifier output, corresponding to a total nonlinear phase shift of 18π. Peak powers of the chirped pulses from the amplifier are up to 57 kW, which corresponds to the generation of largest nonlinear phase shifts from a fiber amplifier while maintaining compressibility to sub-200 fs, in addition to being the highest peak powers obtained from an all-fiber-integrated amplifier, to the best of our knowledge. Numerical simulations provide better agreement with experiments compared with prior reports and give insight into the trade-offs of nonlinear fiber CPA systems.

The experimental arrangement of the laser system is shown in Fig. 1. The seed pulses are generated from a Yb-doped fiber laser oscillator similar to that in [10]. The fiber section of the Yb laser oscillator consists of 6.6 m of single-mode fiber (SMF) (HI-1060) and 0.30 m of Yb-doped fiber, followed by another 0.93 m of SMF. The total dispersion of the cavity is calculated to be about 6150 fs^2. The gain fiber is pumped in-core by a 976 nm fiber-coupled pump diode with an output power up to 550 mW. The pump light is delivered via a 980/1030 nm wavelength division multiplexer. An optical isolator ensures unidirectional operation, which facilitates self-starting operation. Mode locking is initiated and stabilized by the nonlinear polarization evolution effect. The laser output is checked against multiple pulsing by way of long-range autocorrelation and 12 GHz bandwidth rf spectral measurements.

The all-fiber-integrated amplifier consists of a fiber-pigtailed acousto-optic modulator (AOM), a fiber

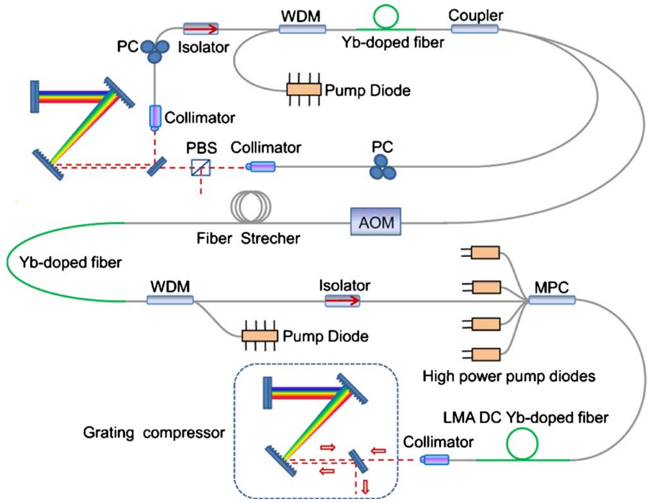

Fig. 1. (Color online) Schematic diagram of the amplifier system. PC, polarization controller; PBS, polarization beam splitter; AOM, acousto-optic modulator; WDM, wavelength-division multiplexer; LMA, large mode area; DC, double-clad; MPC, multiport pump-signal combiner.

stretcher, a core-pumped preamplifier, and a cladding-pumped power amplifier. Finally, the amplified pulses are compressed in a grating compressor. All pump light is delivered through fiber couplers. The preamplifier consists of a 0.30-m-long Yb-doped fiber (of the same type as in the oscillator) pumped backward with a 300 mW pump diode. The power amplifier is pumped codirectionally to protect the pump diodes from optical damage. Pump and signal delivery to the gain fiber is accomplished with a multiport pump-signal combiner (MPC). Four 975 nm diodes, each with up to 10 W power coupled to a 105-μm-core multimode fiber, are used as pump. The amplifier consists of 2-m-long, large-mode-area (LMA), double-clad (DC) ytterbium-doped fiber with a 20 μm core with NA of 0.06, and a 125 μm cladding with NA of 0.46. The output is taken through a fiber-pigtailed isolator-collimator device with a transmission ratio of 90%.

The fiber laser oscillator produces 3-ps-long chirped pulses with a bandwidth of 45 nm at a repetition rate of 28 MHz [Fig. 2(a)]. An output power of 105 mW seeds the amplifier directly through a 50% output coupler placed after the gain fiber and traverses the fiber-integrated AOM, reducing the repetition rate to 1 MHz. The pulses are then stretched to ~150 ps in a 100-m-long fiber stretcher [comprising HI-1060, with an estimated group velocity dispersion of 22 fs^2/mm and third-order dispersion (TOD) of 74 fs^3/mm] and amplified to 104 nJ in the preamplifier. The FWHM bandwidth of the spectrum is measured to be about 20 nm [Fig. 2(b)]. The temporal width, which is also reduced owing to gain narrowing, is measured to be ~80 ps using a 20 GHz bandwidth sampling scope and a fast detector with a rise time of 35 ps [Fig. 2(d)]. The 50% reduction in the pulse duration is due to the dominance of the gain filtering in the preamplifier over self-phase modulation (SPM). The situation is reversed in the power amplifier.

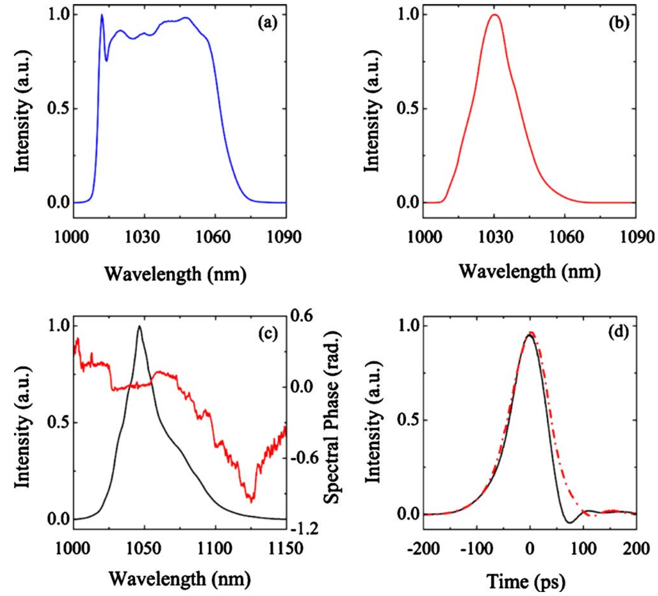

Fig. 2. (Color online) Measured spectra of the pulse from (a) the oscillator, (b) the preamplifier, and (c) the power amplifier at 3.1 W of average power (black curve). Retrieved spectral phase using the PICASO algorithm (jagged curve). (d) Measured pulse duration from the preamplifier (red dashed-dotted curve) and the power amplifier (black solid curve).

Numerical simulations of the pulse generation and amplification based on the model described in [9] guide the experiments at all stages. As can be seen in Fig. 3(a), experimentally the compressed pulse width decreases from 350 to 150 fs with increasing pulse energy from 0.5 to 3 μJ as a result of the compensation of TOD by SPM, and as supported by numerical simulations [Figs. 3(a) and 3(b)]. The broadening mechanism at the long wavelength edge of the spectrum is attributed to the Raman effect, which occurs mainly in the 75-cm-long undoped lead fiber of the collimator, where more than half of the nonlinear phase shift is accumulated. This has been confirmed by observing reduction of the Raman effect by reducing the undoped fiber length, while keeping the total nonlinear phase shift fixed. The Raman amplification is suppressed by the gain filtering during amplification. This likely explains the absence of Raman shifts

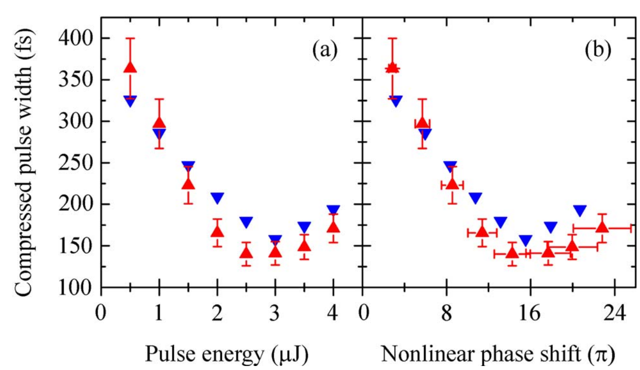

Fig. 3. (Color online) Variation of the compressed pulse width as a function of (a) pulse energy and (b) total nonlinear phase shift in the power amplifier. Triangles pointing up (down) are experimental (simulated) results.

in reports on fiber amplifiers based on rod-type fibers and other photonic crystal fibers, where the output is taken directly out of the amplifier [7,8]. The Raman-amplified spectral components acquire an irregular phase shift [11], which is not straightforward to compensate, leading to accelerated deviation from the transform limit at higher energies. While the use of a fiber-coupled isolator–collimator component is essential for robust operation and to prevent backcoupling of light during, for example, material processing, it enhances the nonlinear effects.

The shortest compressed pulses are obtained in the 2.5–3.1 μJ range with the corresponding nonlinear phase shift of 14–18π. At 3.1 μJ of pulse energy, the spectral width is about 25 nm [Fig. 2(c)]. The pulses are compressed with FWHM durations of 140 fs and 170 fs at 3.1 μJ and 4.0 μJ, respectively, as inferred from the autocorrelation and optical spectrum measurements using the PICASO algorithm [12] (Fig. 4). The simulated and experimental time-bandwidth products are, respectively, 0.90 and 0.92 at 3.1 J, and 1.14 and 1.25 at 4.0 J. The efficiency of our grating compressor is fairly low, at 33%, resulting in a compressed pulse energy of 1 μJ. The peak power is estimated to be ~4.6 MW by integrating the portion of the energy inside the pedestal in the retrieved pulse. 10 MW of peak power should be attainable with the use of higher-quality gratings.

In conclusion, we have demonstrated an all-fiber-integrated amplifier, implementing nonlinear CPA,

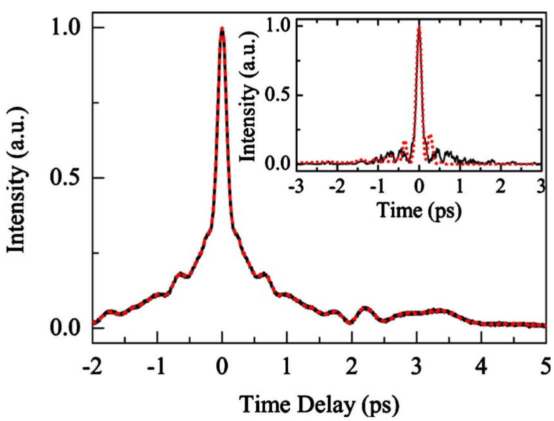

Fig. 4. (Color online) Intensity autocorrelation (black solid curve) and autocorrelation of the retrieved pulse (red dashed curve) of the compressed pulse at 3.1 W output from the power amplifier. Inset, retrieved pulse shape using the PICASO algorithm based on the experimental autocorrelation and spectrum measurements (black solid curve), simulated pulse form (red dotted curve).

with no free-space pump or signal-beam propagation. Thus the amplifier is misalignment free and completely robust and is routinely being used for material processing in our laboratory. It produces 70-ps-long pulses with up to 4 μJ of pulse energy, 57 kW of peak power, and total nonlinear shift of ~22π at 1 MHz repetition rate. These are the highest peak power, pulse energy, and nonlinear phase shifts reported thus far from an all-fiber-integrated amplifier, to our knowledge. The chirped pulses from the amplifier are compressible to 140 fs and 170 fs duration at 3.1 μJ and 4.0 μJ of amplifier output energy, respectively. Intrapulse Raman amplification in the undoped lead fiber of the collimator–isolator device after the gain fiber limits compressibility and increases the pedestal at higher pulse energies. The absence of Raman-shifted components in previous reports on nonlinear fiber CPA systems is attributed to gain filtering during amplification and no subsequent propagation in undoped fiber.

This work was supported by TÜBİTAK under grants 106T017 and 106G089, Marie Curie IRG FiberLaser, Bilkent University Research Funds, and by the Distinguished Young Scientist Award of the TÜBA.

References

1. S. Hädrich, J. Rothhardt, T. Eidam, J. Limpert, and A. Tünnermann, Opt. Express **17**, 3913 (2009).
2. F. Ö. Ilday and F. W. Wise, J. Opt. Soc. Am. B **19**, 470 (2002).
3. T. Schreiber, D. Schimpf, D. Müller, F. Röser, J. Limpert, and A. Tünnermann, J. Opt. Soc. Am. B **24**, 1809 (2007).
4. S. Zhou, L. Kuznetsova, A. Chong, and F. W. Wise, Opt. Express **13**, 4869 (2005).
5. L. Shah, Z. Liu, I. Hartl, G. Imeshev, G. C. Cho, and M. E. Fermann, Opt. Express **13**, 4717 (2005).
6. A. Chong, L. Kuznetsova, and F. W. Wise, J. Opt. Soc. Am. B **24**, 1815 (2007).
7. L. Kuznetsova and F. W. Wise, Opt. Lett. **32**, 2671 (2007).
8. Y. Zaouter, J. Boullet, E. Mottay, and E. Cormier, Opt. Lett. **33**, 1527 (2008).
9. P. K. Mukhopadhyay, K. Özgören, I. L. Budunoglu, and F. Ö. Ilday, IEEE J. Sel. Top. Quant. **15**, 145 (2009).
10. F. O. Ilday, H. Lim, J. R. Buckley, F. W. Wise, and W. G. Clark, Opt. Lett. **28**, 1365 (2003).
11. C. Headley III and G. P. Agrawal, J. Opt. Soc. Am. B **13**, 2170 (1996).
12. J. W. Nicholson, J. Jasapara, W. Rudolph, F. G. Omenetto, and A. J. Taylor, Opt. Lett. **24**, 1774 (1999).